Cell Transit Analysis of Ligand-Induced Stiffening of Polymorphonuclear Leukocytes

Ralph Nossal
Laboratory of Integrative and Medical Biophysics, National Institute of Child Health and Human Development, National Institutes of Health, Bethesda, Maryland 20892 USA

ABSTRACT A mathematical treatment of the mechanical behavior of transiently bonded polymer networks is used to interpret measurements of the pressure-induced passage of pliant cells through microporous membranes. Cell transit times are inferred to be proportional to the instantaneous shear modulus of the cell cortex, a parameter that we then relate to properties of the cortical F-actin matrix. These theoretical results are used to analyze published data on chemoattractant-induced changes of rigidity of polymorphonuclear leukocytes. We thereby rationalize previously noted, peculiar, power-law logarithmic dependences of transit time on ligand concentration. As a consequence, we are able to deduce a linear relationship between the extent of F-actin polymerization and the logarithm of the chemoattractant concentration. The latter is examined with regard to the G-protein activation that is known to occur when chemoattractants bind to receptors on the surfaces of polymorphonuclear cells.

INTRODUCTION

When a neutrophil (PMN cell) is immersed in a medium containing a chemotaxin (i.e., chemoattractant) such as *N*-formyl-methionyl-leucyl-phenylalanine (fMLP), cellular reactions take place that lead to the rapid polymerization of actin filaments (Wallace et al., 1984; Howard and Oresajo, 1985a; Sklar et al., 1985; Coates et al., 1992) along with an increase in cell rigidity (Worthen et al., 1989; Frank, 1990; Pécsvárady et al., 1992). Two techniques have been used to quantitate cell stiffening when neutrophils are placed in a uniform bath of chemotaxin. One, which provides a direct assessment of mechanical rigidity of the cell cortex, uses a miniature "cell poker" to measure the distortions caused by pressing a small glass bead against a cell surface (Worthen et al., 1989). This method, in which forces are applied over an area of only a few square microns, has the advantage that specific, localized regions of a cell can be examined. Results are readily interpretable, yielding a rigidity index defined as the ratio of the applied force to the resultant cell surface depression. However, because cells are examined one at a time, studies involving the cell poker are rather laborious, and one finds that the technique is not particularly useful for kinetic studies. The other method, employing a cell transit analyzer (CTA), quantifies cell rigidity in terms of the time taken for cells to be forced across a microporous filter by hydrostatic pressure (Frank and Tsai, 1990; Pécsvárady et al., 1992). Rapid measurement of the responses of a large group of cells is possible when using this technique, which has been applied successfully to studies of the kinetics of cell activation. Yet, until now, there has been no detailed exposition of the manner in which the transit time (TT) through the filter is linked to the structural properties of the cell. A principal purpose of the present study is to establish this connection.

Both methods indicate that induced cell response varies as a power function of the logarithm of the applied chemotaxin concentration. In particular, when using the CTA, one finds (see below) that measurements (Péscvárady, et al., 1992) of early-stage cell activation indicate an approximately square-law dependence on the logarithm of the stimulus (i.e., $\{\text{Transit time}\} \propto [\log C_L]^{2+}$, where C_L represents the concentration of ligand in the bathing medium). Such power law behavior is somewhat unusual, and it is something of a challenge to understand its origin, which is one of the goals of this investigation. However, it first is necessary to determine how TTs measured by the CTA depend on cell rigidity, particularly as related to changes in the mechanical properties of the cell cytoskeleton.

For this purpose we build on an earlier analysis (Yeung and Evans, 1989) that describes the rate at which pliant cells enter and pass through narrow pores when pushed by hydrostatic pressure. We derive a relationship that links the TT to the cortical dissipation of a composite cell and, by introducing notions of transient polymer networks (Green and Tobolsky, 1946; Doi and Edwards, 1986), we are able to infer, at least for the early stages of cell activation, that the TT is proportional to the instantaneous shear modulus, g_0, of the cortical F-actin matrix. Measurements of cell deformability thus can be analyzed in terms of mathematical theories that relate the elasticity of random actin networks to such factors as total actin concentration, polymerization rate, cross-link density, nucleation kinetics, and capping dynamics. These theoretical considerations lead us to predict that the TT will vary, asymptotically, as the square (or slightly higher power) of the F-actin concentration, i.e., $\{\text{Transit time}\} \propto g_0 \propto [\text{F-actin}]^{2+}$. Consequently, it follows from the discussion in the previous paragraph that cortical

Received for publication 19 November 1997 and in final form 13 June 1998.

Address reprint requests to Dr. Ralph J. Nossal, National Institutes of Health, Bldg. 12A, Rm. 2043, Bethesda, MD 20892. Tel.: 301-435-9233; Fax: 301-402-4544; E-mail: rjn@cu.nih.gov.

© 1998 by the Biophysical Society

0006-3495/98/09/1541/12 $2.00

F-actin content varies linearly with log C_L, i.e., [F-actin] $\propto$ log C_L. Not only is this observation of intrinsic interest, but it supports the likelihood that our analysis of the TT assay is correct, as a similar relationship can be perceived from direct quantification of F-actin concentration (see below).

In the next section (Background), we briefly describe the operation of the cell transit analyzer, examine data relating to the way that chemotaxins affect measured TT, and discuss the theoretical basis for understanding how the passage of a polymorphonuclear (PMN) cell through a pore is related to underlying cell mechanics. We follow this (Further Analysis) by adapting a simplified theory of network elasticity (Nossal, 1988) to relate measured TTs to the amounts of actin incorporated into the cytoskeletal meshwork of the cell. We also show how the theory can guide analysis of the early time rigidity increase noted after cells are activated, and illustrate how these theoretical inferences might be applied to studies of the kinetics of cell activation as well as to more usual cases, in which one determines dose-response relationships.

We continue with some considerations of ligand-binding theory and an examination of the link between the activation of heterotrimeric G-proteins and the growth of the actin cytoskeleton. Mathematical analyses of the activation of heterotrimeric G-proteins by ligand-receptor binding, carried out by other investigators (Mahama and Linderman, 1994; 1995), show that the steady-state concentration of G_α-GTP subunits can vary, like the polymerization of F-actin, proportionally with the logarithm of the chemotaxin concentration over a broad range of ligand concentrations. We discuss the implications of these observations, including the possibility that the transient polymerization of cortical F-actin is linked in a linear fashion to the level of activated G-protein subunits. Finally, we summarize our analysis and discuss its limitations and possible extensions. Mathematical details are presented in various appendices.

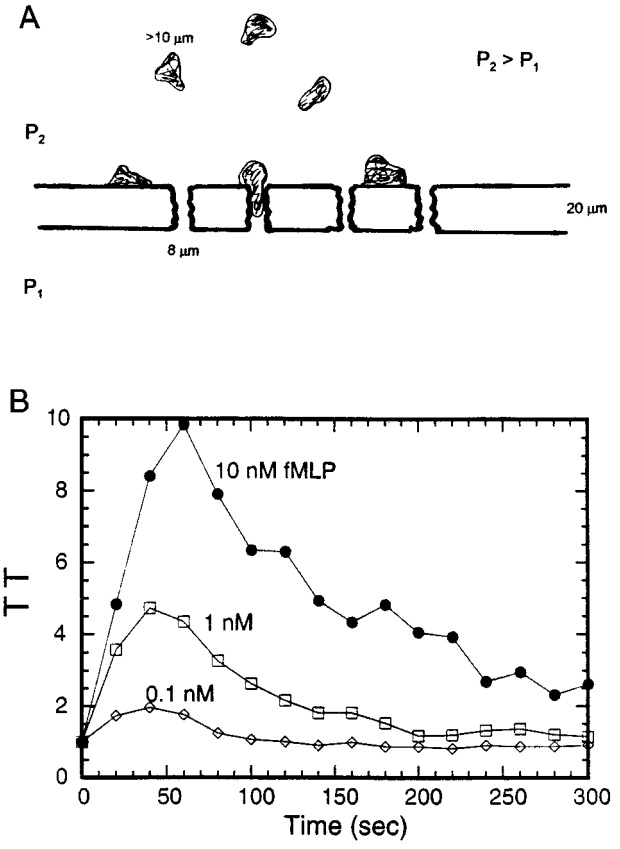

FIGURE 1 Measurement of TT of PMN neutrophils passing through microporous filters. (*A*) Schematic diagram showing cells being pushed through filter by hydrostatic pressure. (*B*) Typical representations of median TTs, determined over 20-s intervals after stimulation by chemotaxin, expressed relative to the median TT of unstimulated cells (the latter being 6–12 ms, depending on sample preparation and filter characteristics). Data taken from Pécsvárady et al. (1992).

BACKGROUND

Cell transit analyzer

Salient features of the CTA are depicted in Fig. 1 *A*. This instrument, which was used first to measure the properties of red blood cells (Koutsouris et al., 1989) and, subsequently, the kinetics of PMN deformability (Frank, 1990; Pécsvárady et al., 1992), uses a polycarbonate membrane, perforated by well-defined pores of narrow size distribution, to separate two reservoirs containing identical buffers. A transmembrane pressure gradient is imposed by maintaining unequal fluid levels in the reservoirs. Cells, suspended in buffer, are placed in the reservoir on the high-pressure side, after which they enter the pores and are pushed across the membrane. The residence of a cell within a pore causes a change in membrane electrical conductance, which provides a measure of the transmembrane TTs of individual cells. The experiments that are analyzed here, which were performed by other investigators (Pécsvárady et al., 1992), utilized a membrane containing pores of mean diameter 8 μm and length 20 μm. The pressure gradient across the membrane was 8 cm H_2O, for which the median TT for unstimulated PMN neutrophils ranged from 6 to 12 ms.

To study the effects of chemotaxins on cell TT, measurements first were made on ~1000 unstimulated cells (Pécsvárady et al., 1992). TTs of cells taken from the same preparation were then determined for 5 min after the cells were activated by suspending them in media containing varying amounts of chemotaxin—either the tripeptide fMLP, or Zymosan-activated plasma (ZAP), which contained the chemotactic factor C5a (details of sample preparation are given in Pécsvárady et al., 1992). The median TTs of cells measured in successive 20-s intervals were expressed relative to the median TTs recorded for unstimulated cells. Typical data are shown in Fig. 1 *B*, where we see that the relative median TT rapidly increases after stimulation, achieving a maximum value at ~60 s, after which the TT decreases in an oscillatory fashion. Furthermore, the maximum value of the relative TT increases when the chemotaxin concentration of the medium in which the cells are immersed is raised. Frank (1990) observed similar be-

havior for PMN leukocytes immersed in 0.1 nM fMLP, when studied with a TT instrument utilizing a polycarbonate filter containing a single 5-μm pore.

Dose response

Representations of the dose-response dependence of the TTs are presented in Fig. 2, where the relative values of TT averaged over the first 60 s after stimulation (TT_{60}) are shown as a function of fMLP concentration. Fig. 2 *A* shows results as published by Pécsvárady et al. (1992), whereas Fig. 2 *B* shows the same data expressed on logarithmic coordinates, that is, $\log(TT_{60} - 1)$ versus $\log(\log[\text{fMLP}] + 11.2)$. (In the latter representation we examine increases in relative TT above the basal value.) The most striking feature of these data is the strong nonlinear dependence on the logarithm of the chemotaxin concentration; by plotting the data in this way, we infer that $(TT_{60} - 1) \propto (\log[\text{fMLP}] + 11.2)^{\alpha}$, where $\alpha \approx 2.2$. (The factor 11.2 is the absolute value of the logarithm of the chemotaxin concentration at which $TT_{60} \cong 1$, i.e., the concentration below which the binding of chemotaxin to a cell surface has no apparent effect on cell rigidity.)

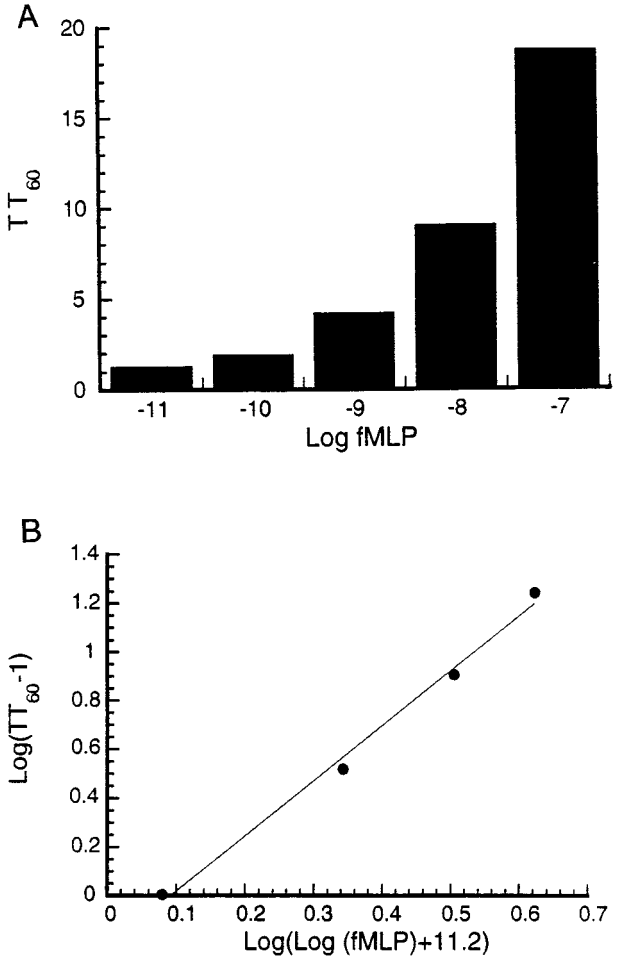

FIGURE 2 Relationship between averaged median TT (TT_{60}; see text) and the logarithm of the chemotaxin concentration (fMLP). (*A*) Dose response as measured by Pécsvárady, et al. (1992). (*B*) The same data, replotted on logarithmic coordinates (see text).

A similarly unusual dependence of PMN mechanical response elicited by fMLP was observed in a related study undertaken by Worthen et al. (1989), which utilized a microscopic cell poker to probe localized cell stiffness. Results of that study also indicated higher order ($\alpha > 1$) dependence on the logarithm of the ligand concentration, although the exact power dependence is difficult to determine because the times, poststimulation, at which the measurements were made were not carefully controlled. Such a higher order response cannot readily be explained merely in terms of chemical reaction kinetics; rather, as shall be shown below, this behavior has its roots in the way the polymerization of actin matrix gives rise to cytoskeletal rigidity.

Other dose-response data, for a different chemotaxin (the C5a complement component present in zymosan-activated plasma), also have been published (Pécsvárady et al., 1992). In addition to determining the relationship between TT_{60} and ligand concentration C_L, the investigators in this case also measured the F-actin content of the cells (using a fluorescent phallacidin assay; Howard and Oresajo, 1985b), 60 s after stimulation with chemotaxin. Originally presented in tabular form (see Table 1), these data now are shown here somewhat differently. In Fig. 3 *A* we present TT_{60} as a function of the square of the relative F-actin concentration (i.e., the ratio of F-actin content to that of unstimulated cells) and discern an asymptotically linear dependence when the F-actin concentration is at least twice that of a critical concentration (the latter is marked by an asterisk in the figure). (The critical concentration is that value of F-actin content below which the TT is the same as that of unstimulated cells, presumably because the concentration of strands in the actin matrix is so dilute that a network does not form sufficiently to offer significant shear resistance.) Fig. 3 *B*, which is also based on the data given in Table 1, shows the related dependence of F-actin content on the concentration of chemotaxin in the bathing medium, from which we directly infer the relationship $[\text{F-actin}] \propto [\log C_L]^{\beta}$ with $\beta \approx 1$. As shall be shown below, the latter serves as a consistency check for our analysis of the TT assay.

TABLE 1 Relations between F-actin polymerization, transit time, and ligand concentration for ZAP-stimulated neutrophils

Dilution ZAP	f	f^2	TT_{60}
1:6400	1.09	1.19	1.04
1:3200	1.40	1.96	1.03
1:1600	1.62	2.62	1.11
1:800	1.93	3.72	1.33
1:400	2.24	5.02	3.23
1:200	2.42	5.86	5.05
1:100	2.55	6.50	6.79

Source: Pécsvárady et al. (1992).
f, F-actin ratio (at 60 s poststimulation, relative to unstimulated cells).
TT_{60}, Cell transit time, average over first 60 s poststimulation.

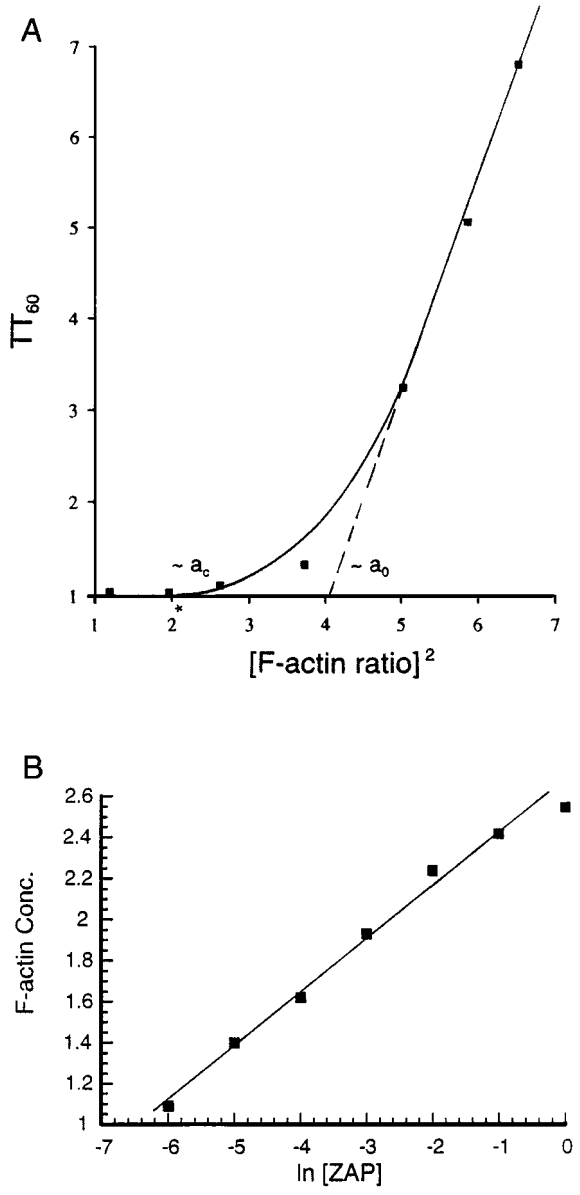

FIGURE 3 Representations of the data given in Table 1 (Pécsvárady et al., 1992), relating to effects of zymosan-activated plasma (ZAP). (*A*) TT_{60} as a function of the square of the ratio of the F-actin content of stimulated cells to that of unstimulated cells, f^2 (see table). A plot of log TT_{60} versus log f (not shown) indicates, more precisely, that in the asymptotic regime $TT_{60} \approx [\text{F-actin}]^z$, where $z \approx 2.2$. (*B*) Relative cellular F-actin content, f, plotted as a function of the logarithm to the base 2 of the dilutions of ZAP-containing plasma given in the first column of Table 1.

Movement of PMN leukocytes into pores

Before continuing, we need to understand how the TT is related to the mechanical properties of the cells. To this end, we use the simplified model of a PMN cell depicted in Fig. 4. This model, introduced by Evans and colleagues (Yeung and Evans, 1989; Evans and Kukan, 1984) to investigate mechanical aspects of the flow of nonadherent cells into micropipettes, considers the cell as a liquid core surrounded by a cortical shell. In its original manifestation the liquid

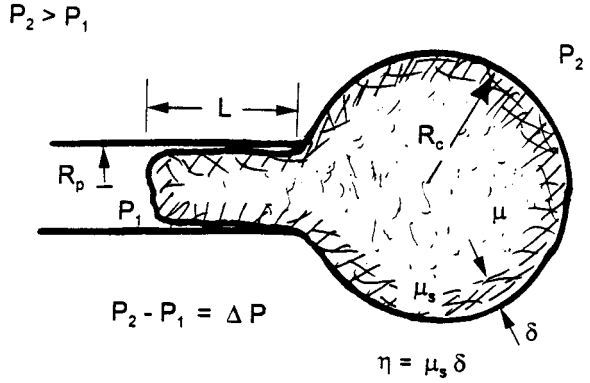

FIGURE 4 Model used to describe the entry of an idealized PMN leukocyte into a micropipette when pushed by hydrostatic pressure (Evans and Yeung, 1989). The viscosity of the liquid core is μ; the equivalent variable for the cortex is $\eta = \mu_s \cdot \delta$, where μ_s is a "surface viscosity" and δ is the cortical thickness. L is the projection length of the cell into the pipette. The radii of the pipette and the cell body are R_p and R_c, respectively.

was taken to be a Newtonian fluid, but later studies (Tsai et al., 1993, 1994) allowed for shear-rate dependence of cytoplasmic viscosity, to account for the apparent non-Newtonian character of the core noted in pipette aspiration experiments when the aspiration pressure is varied. Two mechanical dissipation parameters characterize this system: μ, which is the viscosity of the incompressible liquid core, and η, which is a dissipation parameter associated with surface shear (in units dyn-sec/cm; i.e., viscosity $\times$ thickness). (In general, a coefficient for surface area dilation would be required, but, by considering the cortex to be an isotropic layer, the viscosities for surface dilation and shear are related by a simple constant ratio, viz., 3:1 (Yeung and Evans, 1989).) The other parameters of importance are the radius of the pipette R_p and that of the cell body R_c, and the pressure difference across the cell, $\Delta P = P_2 - P_1$. Although this idealization ignores the internal structure of the granulocyte—most notably the cell nucleus—and assumes a distinguishable boundary between interior core and cell cortex, it has been successfully used to describe several significant features noted when neutrophils enter and move into narrow-bore pipettes.

The mathematical analysis of the model, which has been worked out elsewhere (Yeung and Evans, 1989; Tsai et al., 1993) for the situation in which the cortical layer is thin, indicates that a critical pressure P_{cr} must be exceeded before a neutrophil will enter the capillary. This feature, which has been observed experimentally (Evans and Yeung, 1989; Tsai et al., 1993, 1994; Zhelev et al., 1994), arises from tension in the submembranous cortical structures. Results for the simplest situation (thin cortex plus Newtonian fluid core) can be expressed in terms of dimensionless quantities, $\xi \equiv (\Delta P - P_{cr})/\mu(\dot{L}/R_p)$ and $\tilde{\eta} \equiv \eta/(\mu \cdot R_c)$ (Yeung and Evans, 1989). The first of these, ξ, is a dimensionless flow resistance for cell entry into the pipette at rate $\dot{L} = dL/dt$, and the second, $\tilde{\eta}$, represents the ratio of energy dissipation in the cortex compared with that of the liquid core. Because

of the Newtonian property of the core liquid, all equations of motion can be reexpressed in universal forms containing the dimensionless variables $\tilde{L} \equiv L/R_p$ and $\tilde{t} \equiv t(\Delta P - P_c)/\mu$, and parameters $\tilde{R}_c \equiv R_c/R_p$ and $\tilde{\eta}$. Previous work showed that the solution of those equations yields the following expression for dimensionless flow resistance (Yeung and Evans, 1989):

$$\xi^{-1} \equiv \mu(\dot{L}/R_p)/(\Delta P - P_{cr}) = f_g(\tilde{R}_c, \tilde{\eta}, \tilde{L}), \qquad (1)$$

where $f_g(\cdot)$ has been determined by numerical computation.

Equation 1 is the starting point for our analysis. This expression, when evaluated for the entry of the cell into the pipette (considered to occur when $L = R_p$), gives rise to the solid lines shown in Fig. 5 (the latter having been taken from Yeung and Evans, 1989). Hence, the numerical calculations show an approximately linear dependence on $\tilde{\eta}$, viz.,

$$\xi \approx \kappa\tilde{\eta}, \qquad (2)$$

where $\kappa \equiv \kappa(R_p; R_c)$ is a constant (for given R_p and R_c). From Eqs. 1 and 2, we thus infer

$$(\dot{L})^{-1} \approx [\kappa(R_p; R_c)] \cdot (\eta/\mu R_c) \cdot \frac{\mu}{R_p(\Delta P - P_{cr})} \approx \frac{\eta\kappa(R_p; R_c)}{R_p R_c(\Delta P - P_{cr})}. \qquad (3)$$

Fig. 5 also shows results (*dotted lines*) of a calculation performed by assuming that the core is inviscid (i.e., $\mu = 0$), from which one observes that, to first order, the cortical resistance is additive to that of the liquid core (Yeung and Evans, 1989).

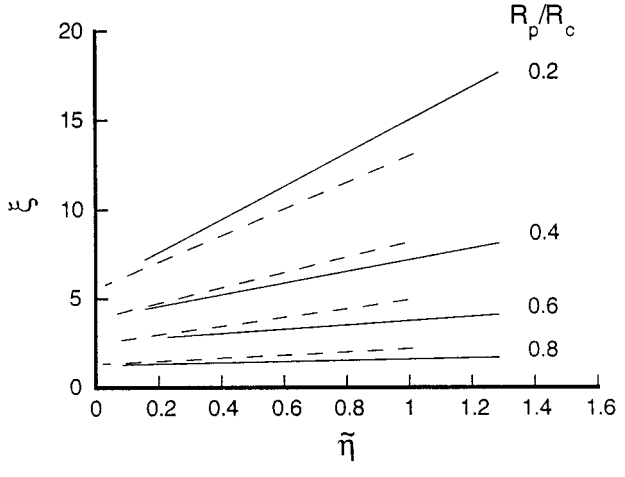

FIGURE 5 Dimensionless flow resistance, ξ, versus cortical dissipation parameter $\tilde{\eta}$ (see text preceding Eq. 1), for different ratios of pipette radius to cell radius, R_p/R_c. (The figure is adapted from Yeung and Evans (1989).) The parameter $\tilde{\eta}$ is the ratio of energy dissipation in the cell cortex to that occurring in the interior of the cell (the "core"). For fixed core viscosity, approximately constant R_c, and fixed pressure across the membrane barrier (see Fig. 1), one infers that the TT varies, approximately, in linear proportion to the mechanical dissipation occurring in the cell cortex (see Eqs. 1–4).

The critical pressure P_{cr} is a function of both the pipette and cell radii, and is given (Yeung and Evans, 1989; Evans and Yeung, 1989) as $P_{cr} = 2\bar{\tau}_0(1/R_p - 1/R_c)$, where $\bar{\tau}_0$ is a persistent cortical tension. Experimental evidence (Evans and Yeung, 1989; Tsai et al., 1993, 1994; Zhelev et al., 1994) indicates that $\bar{\tau}_0$ is on the order of 0.03–0.05 dyn/cm for unstimulated PMN cells. Consequently, for the conditions used in the TT experiments ($R_p \approx 4$ μm, $\Delta P = 8$ cm $H_2O \approx 10^{15}$ dyn/cm^2), one finds $P_{cr} \ll \Delta P$, so the term P_{cr} appearing in Eq. 3 may be neglected. Furthermore, because of the relatively large diameter of the membrane pores (as compared with the radius of an equivalent spherical PMN cell), one can assume R_c to be essentially unchanging as a cell enters a pore. Hence, the transit time of an average cell moving through a typical pore of length $\mathcal{L}$ (where $\mathcal{L}$ is on the order of a few times R_c) can be expressed as

$$\{\text{transit time}\} \approx \mathcal{L}/\dot{L} \approx \left[\frac{\kappa(R_p; R_c) \cdot \mathcal{L}}{R_p R_c \Delta P}\right] \cdot \eta,$$

where the term in brackets is a constant. It follows that the relative TT is given simply as

$$\text{TT} \approx \eta/\eta_0, \qquad (4)$$

where η_0 is a reference value of cortical resistance (e.g., that for unstimulated cells). This relationship is a key to understanding how the TT assay can be used to study cell activation kinetics.

The relationship given by Eq. 4, which is a new deduction, is intuitively reasonable. When a PMN cell moves into a pore, its membrane unfolds as the cell changes shape from a sphere (whose membrane is highly convoluted) to a more oblong-shaped entity. Even for the large-pore membranes used in the CTA experiments that we are analyzing, the extension of the cell surface while in the pore is at least 10%. Consider, for example, 8-μm-diameter pores of length 20 μm, and suppose that an 8.5^+ μm diameter spherical PMN cell, when in a pore, takes the form of a cylinder of volume equal to that of the round cell; the radius of this cylinder is $\sim 0.9 \times R_c$ and its length is h, where the constant volume requirement implies $h/R_p \approx 1.8$ for the ratio of cylinder length to pore radius, leading to the result $A_{cyl}/A_{sph} \approx 1.1$. Moreover, we note that the inferred value for h/R_p is close to the ratio of pore length to pore radius, from which we conclude that shortly after a cell has completed its entry into the pore on the high-pressure side of the membrane, it begins to leave the pore on the low-pressure side. Hence, for almost the entire time that a cell is in a pore, the kinetics of cell distortion are principally those of cell surface dilation, which, in turn, depends on the properties of the underlying cortical cytoskeleton.

Furthermore, fluorescent studies of the organization of F-actin within suspended, spherical PMN cells stimulated by chemotactic peptide are in accord with Eq. 4. These studies show that F-actin first polymerizes at the cell periphery (Wallace et al., 1984; Coates et al., 1992). The F-actin distribution is symmetrical for 30–45 s and then

becomes asymmetrical as the cells start to develop discernible polarity, even while the cells remain round (Coates et al., 1992). (The distribution becomes diffuse only after ~1 min.) Moreover, although cell response can be influenced by preincubation with phorbol ester (Wymann et al., 1989) or factors that inhibit actin polymerization (Watts et al., 1991), total F-actin content is seen to peak at roughly the same time as the signal recorded in turbidity measurements (Sklar et al., 1985). The development of rigidity in fMLP-stimulated cells follows similar kinetics (see Fig. 1 *B*), which itself strongly suggests that changes in cortical F-actin structures are involved in the observed mechanical response.

Other evidence for the existence of a definable cell cortex in PMN cells has come from both ultrastructural and mechanical studies. Transmission electron microscopy of unstimulated PMN cells indicates a relatively thin, random meshwork lying adjacent to the cell membrane. This layer has a thickness of 0.1–0.2 μm (Sheterline and Rickard, 1989), similar to that seen in other blood leukocytes (Bray et al., 1986). The previously mentioned mechanical studies involving micropipettes (Evans and Yeung, 1989; Tsai et al., 1993, 1994; Zhelev et al., 1994) all are consistent with the notion that a demarcation exists between a thin cortical shell and the cell interior. Furthermore, estimates based on measurements with small pipettes (Zhelev et al., 1994) indicate that the bending modulus of the cortex is an order of magnitude greater than that of a bare bilayer membrane. We shall see, below, that the CTA-measured, chemotaxin-stimulated, rapid increase in cell rigidity quantitatively agrees with the notion that the F-actin concentration increases within a cortical region of essentially fixed thickness.

Before concluding this section, it should be noted that were structural changes of the cell cortex to vary strictly in proportion to changes in the interior of the cell (such that $\eta/(\mu \cdot R_c) = \text{constant}$), analysis based on Eq. 3 would yield $(\dot{L})^{-1} \propto \mu$. In essence, this result is equivalent to one derived by Needham and Hochmuth (1990) for a model of a semispherical liquid drop with surface dissipation, obtained as a limiting case of the Yeung and Evans model. One then would find TT $\propto \mu/\mu_0$, where μ is the viscosity of the fluid core, and a different interpretation of experimental results would be required. However, although there is no a priori way to determine which view of cell activation is correct, i.e., whether the change in rigidity is due to changes in the elasticity of the cortex or changes in the cell interior, the similarity between the time scale of cortical actin polymerization and the development of rigidity shown in Fig. 1 suggests that the cortex must be involved in a significant way.

Moreover, a cell, even when in suspension, might develop F-actin-rich ruffles at its surface when stimulated by chemotactic factor, in which case the notion of a smooth cell with a well-defined cortex might have to be modified. Thus it might be of interest to rework the Yeung and Evans model to deal with irregularly shaped cells that have a thick cortex and whose features are explicitly accounted for when considering surface dilations. Furthermore, the simple picture shown in Fig. 1 *A* may have to be changed, in that the cell might be flattened somewhat against the filter before being pushed through a pore. However, such modifications are beyond the scope of this investigation, and probably would be meaningful only if more refined data sets were made available. Regardless, to the extent that Eq. 2 is a good approximation (which may have generality beyond the simplified model), one can infer Eq. 4. The latter seems to be consistent with the data analysis that follows.

ADDITIONAL ANALYSIS

Network elasticity

The cortical cytoskeleton of a PMN leukocyte is a labile structure whose mechanical rigidity largely depends on the interactions between F-actin strands. In some cases these interactions are entanglements, in which case the junctions between two intersecting F-actin filaments are said to have a "functionality" of four (i.e., there are four "strands" leading away from the junction). In addition, the F-actin filaments may be cross-linked by actin-associated proteins that interact with the actin chains via reversible, noncovalent bonds (see, e.g., Alberts et al., 1994, for further discussion).

Because of the transient nature of such interactions, the internal connections within the actin network may change while the network is subjected to slow strains, in which case the cortex will behave as if it were a highly viscous fluid. However, when subject to very rapid distortion, the cortical matrix will appear more like an elastic material. These behaviors are illustrated by studies on F-actin networks stabilized by the actin-binding proteins α-actinin (Sato et al., 1987) and filamin (Janmey et al., 1990). Gels cross-linked by α-actinin, when subjected to sinusoidal perturbations whose frequencies fall into the range 10^{-4}–10^{0} Hz, exhibit a complex, frequency-dependent, elastic modulus that tends at extremely low frequencies to a value close to that of a solution of unadorned actin filaments (lacking α-actinin) (Sato et al., 1987). Such observations, augmented by complementary studies of the temperature dependence of rate constants (Sato et al., 1987), lead to the conclusion that the interactions between actin and α-actinin have a high probability of being interrupted during the course of the perturbation. A similar behavior is expected for gels temporarily stabilized by entanglements.

The simplest description of such "transient-gel" mechanical behavior (see Appendix A) derives from a model whose chain interactions and, therefore, viscoelastic response are characterized by a single relaxation time (Green and Tobolsky, 1946). In this case, if a material is subjected to a weak strain $\gamma(t)$ that is periodic in time such that $\gamma(t) \approx \sin \omega t$, the resulting stress will vary (Ferry, 1980) as $\sigma(t) \approx [\tilde{G}'(\omega)\sin \omega t + \tilde{G}''(\omega)\cos \omega t]$. For sufficiently low frequencies one finds $\tilde{G}'(\omega) \approx 0$ and $\tilde{G}''(\omega) \approx g_0 \omega \bar{\lambda}^{-1}$, where $\bar{\lambda}^{-1}$ is an average relaxation time and g_0 is an instantaneous, high-frequency, elastic shear modulus (see Appendix A).

Hence, for slow distortions, the material behaves like a viscous, dissipative substance whose viscosity is given by

$$\eta = g_0/\bar{\lambda}. \tag{5}$$

Thus, because the average relaxation time associated with individual filament-filament interactions will not change significantly when a cell is stimulated by chemotaxin, it follows from Eqs. 4 and 5 that the TT varies in proportion to the instantaneous shear modulus, i.e.,

$$\mathrm{TT} \propto g_0. \tag{6}$$

In principle, g_0 can be related, by an appropriate theory of elastic response, to the microscopic attributes of the cytoskeletal matrix, including the length and rigidity of individual filaments and the number and nature of the filament-filament interactions.

The theory needed to describe the elastic properties of real, complex polymer networks (e.g., networks composed of stiff polymers, and/or containing dangling strands, etc.) still is only partially developed, so for present purposes we use an expression based on the classical theory of rubber elasticity (Flory, 1953; Pearson and Graessley, 1978). When cross-link densities are much greater than a minimal, critical value, a_c, the theory of rubber elasticity relates the modulus g_0 to the number of chains in the network N, the network volume V_0, and the fraction of elemental chain units (e.g., monomers) directly participating in the cross-linking reactions a, as (Pearson and Graessley, 1978; Nossal, 1988)

$$g_0 \sim g_0^{\text{asymp.}} \equiv \left(\frac{a - a_0}{a_0}\right)\frac{N}{V_0}\Phi k_B T \qquad (a \gg a_c). \tag{7}$$

In this expression, Φ is a constant of order 1, k_B is Boltzmann's constant, and T is the temperature. The term a_0 is a constant that is related to the average length of the filaments, being proportional to a_c according to an expression that depends on the nature of the junctions that hold the chains together (viz., the junction "functionality"). The derivation of Eq. 7 neglects possible effects of dangling polymer chains, and is based on an assumption that the polymer chains are randomly oriented, have zero persistence length, and can pass through one another. Furthermore, only the entropic component of the modulus is accounted for by this treatment, but we later discuss related work (MacKintosh et al., 1995) that takes into account the inherent stiffness of the actin filaments. Although clearly an idealization, the expression given by Eq. 7 nonetheless often serves successfully as a first approximation to describe network properties.

For networks cross-linked by filamin molecules or transiently stabilized by entanglements, which both form junctions between two F-actin filaments, one anticipates $a_0 \approx 2a_c$ (see Appendix B). In such an instance one can show (Nossal, 1988) that g_0 may be rewritten as

$$g_0^{\text{asymp.}} = (\mathcal{A} - N)\Phi k_B T/V_0, \tag{8}$$

where $\mathcal{A}$ is the number of junctions in volume V_0. By considering the stoichiometry of binding and by assuming that the effective association constants for junction formation are low (as should be the case for entanglements), one can further demonstrate (see Appendix B) that Eq. 8 leads to

$$g_0^{\text{asymp.}} \approx [\epsilon(\Delta C)^z - N]\Phi k_B T/V_0 \sim (\Delta C)^z \qquad (a \gg a_c), \tag{9}$$

where ϵ is a constant and ΔC represents the amount of material in the lattice—i.e., the amount of actin that has been incorporated into filaments.

The term $(\Delta C)^z$ is proportional to the number of junctions (e.g., the number of entanglement points). A simplified, idealized calculation for "Gaussian chains" (Flory, 1953) leads to the value $z = 2$ (for "phantom networks," in which the chains are allowed to cross each other), and a more complicated calculation predicts $z = 9/4 = 2.25$ (when excluded volume is taken into account). Yet another calculation (MacKintosh et al., 1995), undertaken to explain the magnitudes of rigidities noted for actin solutions by allowing for internal stiffness of F-actin filaments, yields an expression that differs somewhat from that given in Eq. 7; however, the dependence of modulus on ΔC is similar, with the predicted value of the exponent being $z = 11/5 = 2.20$. The main point is that Eqs. 6 and 9 imply that the TT should vary, asymptotically, as

$$\mathrm{TT} \propto (\Delta C)^z, \tag{10}$$

where $z \approx 2.0$–2.2.

Comparison with the data shown in Fig. 3 *A* now can be made. We see that the TT (i.e., the instantaneous elastic shear modulus) varies asymptotically as a power of the F-actin concentration, $[\text{F-actin}]^z$, where in accordance with Eqs. 9 and 10, the exponent is observed to be $z \approx 2^+$. Moreover, the extrapolated intercept a_0 is approximately twice the apparent critical cross-link concentration a_c. This observation supports the notion that the rigidity increase occurring upon chemotaxin stimulation is primarily due to an increase in F-actin concentration, which results in an increased number of sites where entanglements or other tetrafunctional junctions can form (see Appendix B). There is no evidence that the nature of the cross-linking changes, for example, because of a change in the concentration or potency of actin-binding proteins. If data similar to those shown in Fig. 3 *A* were to be acquired on a finer scale (i.e., at more closely spaced values of chemotaxin concentration; see Table 1), one might be able to distinguish more clearly between an exponent of value $z \approx 2.0$ and one of value $z \approx 2.25$. One probably also would be able to rule out the bundling of filaments as a contributor to early stiffening of cells (see Appendix B).

Early kinetics of PMN mechanical response

One advantage of the CTA is that data such as those shown in Fig. 1 *B* can be used to investigate kinetic aspects of cell

activation. In particular, the early response measured in the TT assay might provide insight into the way in which actin monomer is made available to increase the number or length of F-actin filaments. Possible mechanisms for increasing filament length include the release of capping protein from preexisting chains, a change in filament assembly/disassembly rate constants (e.g., due to a change in nucleotide binding), and the release of sequestered G-actin from actin-bound storage assemblies (Pantaloni and Carlier, 1993; Machesky and Pollard, 1993; Fechheimer and Zigmond, 1993; Theriot, 1994). In each case the starting point for analysis is Eq. 10, which indicates that the TT can be expressed approximately as

$$\mathrm{TT} \propto (\Delta C)^2 \approx (C_\mathrm{T} - C_1(t))^2, \tag{11}$$

where C_T is the total actin concentration and $C_1(t)$ represents the nonincorporated, free actin concentration.

The kinetic equation for $C_1(t)$ has a simple form if the rate constants for the addition of free monomers to preexisting chains do not depend on chain length, which is an oft-made assumption. In such a case one has, simply,

$$\frac{\mathrm{d}C_1}{\mathrm{d}t} = -(k^+C_1 - k^-)N + S(t), \tag{12}$$

where N is the number of F-actin chains (that is, polymers containing actin monomers in excess of those, e.g., 3 or 4, needed to form a nucleation seed), and $S(t)$ is a source term for free actin monomer. Suppose, further, that the number of actin chains is a fixed value, N_0, and that the source term is $S(t) = C_1(0)\delta(t)$, i.e., that the sample initially contains unpolymerized actin of concentration $C_1(0)$ and that no other actin is added to the system. Equation 12 then has the solution

$$C_1(t) = K^\mathrm{D} + (C_1(0) - K^\mathrm{D})e^{-k^+N_0t}, \tag{13}$$

where $K^\mathrm{D} \equiv k^-/k^+$ is the dissociation constant for monomer-polymer interactions. From Eq. 13 we see that, at long times, $C_1(t)$ tends to a limiting value $C_1^\infty = K^\mathrm{D}$, and the amount of actin present as F-actin tends to the "equilibrium value," $\Delta C^\infty = C_\mathrm{T} - C_1^\infty = C_\mathrm{T} - K_\mathrm{D}$.

Let us now consider what would happen if, after such equilibrium were established, the pool of polymerizable actin were to be rapidly increased. Suppose, for example, that G-actin were released from an association with thymosin β4 (Nachmias, 1993) as a result of cell activation. In this instance the solution of Eq. 12 again yields the expression given by Eq. 13, except that $C_1(0)$ is replaced by $C_1(0) = K^\mathrm{D} + \delta C$, where δC is the amount of newly released G-actin. That is, the amount of actin incorporated into polymer chains increases with time, to a value commensurate with the new effective total actin concentration, C_T^N (the new concentration of nonsequestered actin). By expanding the exponent in Eq. 13 and performing some algebra, one finds that the kinetics of F-actin polymerization may be expressed as

$$\begin{aligned}\Delta C(t) &= C_\mathrm{T}^\mathrm{N} - C_1(t) \\ &= (C_\mathrm{T}^0 - K^\mathrm{D})\left[1 + \frac{\delta C}{(C_\mathrm{T}^0 - K^\mathrm{D})}k^+N_0t + \cdots\right],\end{aligned} \tag{14}$$

where $(C_\mathrm{T}^0 - K^\mathrm{D}) \equiv \Delta C_0$ is the amount of actin incorporated into polymer chains before the release of additional actin from previously inactive complex. Thus it follows from Eq. 11 that, after activation at time $t = 0$, the TT is given as

$$\mathrm{TT} = \mathrm{TT_b}\left(1 + 2\frac{\delta C}{\Delta C_0}k^+N_0t + \cdots\right), \tag{15}$$

where $\mathrm{TT_b} \propto (C_\mathrm{T}^0 - K^\mathrm{D})^2$ represents a basal value (the TT for unstimulated cells).

Equation 15 predicts that the TT measured after release of sequestered G-actin should increase linearly with time, as indeed is seen in the data presented in Fig. 1 *B*. To obtain the expression given in Eq. 15, we have assumed that the kinetic processes of actin polymerization are much slower than other steps in the transduction process, i.e., that on the time scale of observation, the release of sequestered actin occurs very rapidly after stimulation by chemotaxin. These calculations, which ignore many complexities, are meant primarily to illustrate how a macroscopic measurement of cell rigidity might shed light on certain mechanistic details of cell activation. Other postulated mechanisms might yield different time dependences, as does, e.g., the rapid uncapping of previously capped chains. (One can show, by a similar but somewhat lengthier calculation, that the latter leads to a t^2 dependence for early TT change.) We also note that the predicted linear time dependence is not specific to the liberation of bound G-actin, but would also be achieved if cell activation were to lead to a rapid change in the kinetic constants for chain polymerization. Recent in vitro studies (Carlier et al., 1997) have shown that the latter can be effected by a change in the phosphorylation state of "actin depolymerizing factor" (cofilin), and it would be interesting to systematically examine this and other kinetic schemes with a view toward defining experimental protocols that might better discriminate between possible mechanisms.

Connection between ligand binding and cytoskeletal polymerization

We still need to explain the dose-response relationship shown in Fig. 2. It has been known for some time that the binding of fMLP and other chemotactic factors to cell surface receptors results in the activation of heterotrimeric G-proteins (Omann et al., 1987), although details of the coupling between this initial transduction step and the polymerization of F-actin are still unclear.

One hypothesis is that the activation of G-proteins leads to an increase in phopholipase C-β, resulting in the hydrolysis of plasmalemma-bound phosphatidylinositol 4,5-bisphosphate (PIP_2) and the concomitant release of PIP_2-

bound profilin (Machesky et al., 1990; Machesky and Pollard, 1993). The liberated profilin might compete with thymosin $\beta 4$ for the G-actin that is stored in the cell in association with thymosin $\beta 4$; the resulting profilin/G-actin complex then would bind to the barbed end of an actin filament, whence the actin monomer is added (Pantaloni and Carlier, 1993). That such linkage exists between the activation of G-proteins and actin polymerization is suggested by the similarity between the dose-response relationship for ligand-induced GTP-bound G_α subunit generation and that for ligand-induced F-actin polymerization uncovered above in our analysis of the data of Pécsvárady et al. (1992).

As described in Appendix C, a simple mathematical model for stimulus transduction by heterotrimeric G-proteins, involving straightforward application of mass action binding kinetics, yields the relationship

$$[\alpha]_{ss} = \frac{1}{\gamma_1 + \gamma_2 e^{-Y}}. \quad (16)$$

Here, $[\alpha]_{ss}$ represents the concentration of activated GTP-G_α subunits (or, similarly, $\beta\gamma$ subunits) induced by ligand in the bathing medium at concentration [L], and the variable Y is defined as $Y = \ln[L]/K_D$, where K_D is the dissociation constant for ligand-receptor binding. The coefficients γ_1 and γ_2 are combinations of the rate constants involved in the G-protein activation cycle (see Appendix C).

We recall that the work of Pécsvárady et al. (1992) showed that [F-actin] $\propto$ log C_L, where C_L is the ligand concentration (see Fig. 3 *B*). The significant point is that the expression given in Eq. 16 also yields an approximately linear relationship between $[\alpha]_{ss}$ and log [L]. Thus one might make the argument that the degree of cortical actin polymerization is directly proportional to the amount of activated G-protein (viz., $[\alpha]_{ss} \propto \log[L]$; [F-actin] $\propto \log[C_L]$; therefore [F-actin] $\propto [\alpha]_{ss}$.)

Whereas the data shown in Fig. 2 show approximately logarithmic responses to occur over approximately four decades of log [L], the relationship between $[\alpha_{ss}]$ and log [L] given by Eq. 16 is linear only over 1.5–2 decades. However, Mahama and Linderman (1994) used Monte Carlo simulations to examine more elaborate models of G-protein activation than the simple bulk reaction model that leads to Eq. 16. By accounting for such factors as receptor diffusivity, possible spatial heterogeneity in the distribution of receptors and released G-protein subunits, and the two-dimensional nature of the ligand-receptor reaction space, they showed that the activation of heterotrimeric G-proteins can depend linearly on the logarithm of the ligand concentration over a much broader range of concentrations than indicated by Eq. 16. Moreover, multiplicity in receptor species (e.g., as evidenced by differing binding constants), receptor inactivation (Mahama and Linderman, 1995), and the precoupling of receptors with G-proteins (Shea and Linderman, 1997) can lead to even greater broadening of the apparent linear-log range. Thus this seeming inconsistency may be more apparent than real.

SUMMARY AND DISCUSSION

Other techniques can be used to study cellular F-actin in situ, including light scattering, fluorescent detection of incorporated phalloidin or phallocidin, and electron microscopy. Among these, only light scattering (Sklar et al., 1985; Wymann et al., 1990) provides a real-time, rapid measure of a change in F-actin content. Moreover, none provide functional information relating to the cell activation that occurs, e.g., as a result of ligand binding. Although it had been established previously that the CTA can be used to obtain qualitative measures of the rigidity of extensible biological cells, the link between measured TTs and intrinsic cell properties was unclear. A primary goal of this work was to establish how the CTA can be used to obtain quantitative parameters that might provide insight in the mechanisms of cell activation. By evaluating previously published data in a self-consistent manner, a clearer picture has now emerged of the type of information that can be obtained from the assay.

As demonstrated above, the CTA provides real-time, integrative information about cell mechanical response that is clearly linked to structural changes in the cell cytoskeleton. We have argued that, to a good approximation, the TT is directly proportional to the viscoelastic dissipation modulus of the cell cortex. It follows that, because of transient-gel characteristics of actin networks, the dissipation modulus can be considered to be proportional to the instantaneous shear modulus of the cortical network (at least for neutrophils). Because the shear modulus of an actin network can be expressed in terms of parameters relating to the microscopic mechanical structure of the network, these observations allow the CTA to be used as a tool to investigate cytoskeletal changes that occur when a cell is stimulated by chemotaxins. In particular, we have inferred that the increase in cell rigidity of PMN cells, noted upon stimulation by chemoattractant, derives primarily from an increase in the density of the F-actin matrix. The increased concentration of F-actin strands results in a concomitant increase in the number of contact points where intrastrand entanglements or tetrafunctional cross-linking can occur. That is, the rigidity increase seems to arise from a change in the amount of polymerized actin, not from an increased potentiation or a greater number of putative cross-linking molecules. However, although these inferences substantiate the notion that the actin cytoskeleton of the cell cortex behaves mechanically like a random polymer network, it is impossible to determine from the TT data whether intrinsic actin strand rigidity (MacKintosh et al., 1995) contributes in an important way to in vivo gel strength.

Cursory kinetic analysis of cell response indicates that F-actin accretion may result from the release of monomeric G-actin from cytoplasmic storage complexes. The data thus

are consistent with a mechanism in which the production of activated subunits of heterotrimeric G-proteins, resulting from binding of chemoattractant molecules to specific receptors, leads to the hydrolysis of PIP_2 and, consequently, the release of profilin that might have been bound to the PIP_2. The newly freed profilin then can bind to G-actin and deliver it to existing F-actin strands, leading to filament elongation (Machesky et al., 1990; Carlier et al., 1997). Although our analysis suggests that the amount of F-actin in the cell cortex is proportional to steady-state G_α-GTP concentration, additional study is required to understand how control loops (Richardson et al., 1996) and other elements of signaling pathways might be involved.

Last, we note that, in various respects, the exposition of cell mechanics carried out in this paper is a small deformation analysis. It succeeds because the average dimensions of the PMN cells are similar to the diameters of the membrane pores that were used to acquire data. If, however, cells must distort to a greater degree to pass through a pore, a more elaborate analysis might be required to account for nonlinear elastic behavior of the cell cortex and other complicated structural attributes of the cells.

APPENDIX A: LINEAR VISCOELASTIC RESPONSE

The linear constitutive relation for viscoelastic response, relating the shear stress $\sigma(t)$ to an imposed shear strain $\gamma(t)$, may be written as

$$\sigma(t) \approx \int_0^t G(t-s)\dot{\gamma}(s)\mathrm{d}s, \tag{A1}$$

where $\dot{\gamma}$ is the time derivative of $\gamma(t)$, and the kernel $G(t)$ represents a time-dependent viscoelastic response function. Suppose that $G(t)$ can be written as

$$G(t) = \sum_i g_i e^{-\lambda_i t} \approx g_0 e^{-\bar{\lambda}t}, \tag{A2}$$

where g_0 and $\bar{\lambda}$ are defined as $g_0 \equiv \Sigma_i g_i$ and $\bar{\lambda} \equiv g_0^{-1}\Sigma_i g_i\lambda_i$. In this case when the strain is periodic in time, e.g.,

$$\gamma(t) \approx \sin \omega t, \tag{A3}$$

one finds that the stress will vary as

$$\sigma(t) \approx [\tilde{G}'(\omega)\sin \omega t + \tilde{G}''(\omega)\cos \omega t], \tag{A4}$$

where $\tilde{G}'$ and $\tilde{G}''$ are given as

$$\tilde{G}'(\omega) = g_0\omega^2(\bar{\lambda}^2 + \omega^2)^{-1}, \qquad \tilde{G}''(\omega) = g_0\bar{\lambda}\omega(\bar{\lambda}^2 + \omega^2)^{-1}. \tag{A5}$$

The "storage modulus" $\tilde{G}'(\omega) \equiv \omega \int_0^\infty \sin \omega t\, G(t)\mathrm{d}t$ represents in-phase, elastic-like response, and the "loss modulus" $\tilde{G}''(\omega) \equiv \omega \int_0^\infty \cos \omega t\, G(t)\mathrm{d}t$ is associated with out-of-phase, viscous-like dissipative behavior.

For rapidly applied perturbations giving rise to high-frequency response, this model behaves like a purely elastic material, i.e., $\tilde{G}'(\omega) \approx g_0 \approx G(0)$ and $\tilde{G}'' \to 0$, where $G(0)$ is the instantaneous response of the material (on the time scale of measurement, i.e., $\bar{\lambda}t \ll 1$). In contrast, as $\omega \to 0$ (low frequency, slow perturbations), Eq. A5 becomes

$$\tilde{G}'(\omega) \approx 0, \qquad \tilde{G}''(\omega) \approx g_0\omega\bar{\lambda}^{-1} \equiv \eta\omega, \tag{A6}$$

where the units of η are those of viscosity.

APPENDIX B: INSTANTANEOUS (HIGH-FREQUENCY) SHEAR MODULUS

The classic theory of rubber elasticity for cross-linked random networks leads to the expression given in Eq. 7, viz.,

$$g_0 \approx g_0^{\text{asymp.}} \equiv \left(\frac{a-a_0}{a_0}\right)\frac{N}{V_0}\Phi k_B T \qquad (a \gg a_c), \tag{B1}$$

where a (the "cross-link density") is the fraction of units in the polymer chains that are directly involved in interchain interactions. (The other variables in this equation are identified in the text.) This expression has been developed for interpenetrating random-coiled chains ("phantom networks"). As a first approximation, it describes the shear elastic modulus of either permanently cross-linked networks or, when subjected to sufficiently rapid perturbations, transient networks stabilized by impermanent interactions.

Although Eq. B1 holds for large values of a, the general behavior of the shear modulus is similar to that shown in Fig. 3 *A*, viz., an asymptotically linear relationship for values of a much greater than a_c, and another behavior tending to zero as a approaches a_c. The quantity a_c may be interpreted as the cross-link density necessary to form a spanning cluster within the network. In general, the extrapolated intercept a_0 is proportional to a_c, the proportionality coefficient being a functional of the fractions $\{\omega_j\}$ of network junctions joining units belonging to j different chains (requiring $j-1$ cross-links). If one defines the quantities f_w and f_n as

$$f_w \equiv 2\sum_{j=2}^{\infty} j\omega_j, \qquad f_n \equiv 2\left(\sum_{j=2}^{\infty} \omega_j/j\right)^{-1}, \tag{B2}$$

then a_0 and a_c are related according to (Nossal, 1985, 1988)

$$a_0 \approx \left[\frac{\frac{1}{2}f_w - 1}{1 - sf_n^{-1}}\right]a_c, \tag{B3}$$

where a_c is given in terms of the average number of monomers in a chain, $\langle r\rangle$, as (Pearson and Graessley, 1978)

$$a_c = [(f_w/2 - 1)(\langle r\rangle - 1)]^{-1}. \tag{B4}$$

For "tetrafunctional junctions," for which $j = 2$, one finds from Eqs. B2 and B3 that $a_0 = 2a_c$. That is, when the shear modulus is asymptotically linear in a variable whose extrapolated intercept is a_0, the modulus will vanish at a value of that variable that is half the extrapolated intercept value.

From Eqs. B3 and B4 one sees that a_0 can be expressed as $a_0 \approx [(1 - 2f_n^{-1})\langle r\rangle]^{-1}$. But the average chain length $\langle r\rangle$ is given as $\langle r\rangle = \Delta C/N$, where ΔC is the amount of actin incorporated into filaments and N represents the number of chains. Note, also, that the fraction of monomer units involved in cross-links is given as $a = (\Sigma jA_j)/\Delta C$, where A_j is the number of junctions linking j chains together. It thus follows that Eq. B1 can be alternatively expressed as

$$g_0 \approx \left(\sum_j jA_j(1 - \sum_\ell w_\ell/\ell) - N\right)\frac{\Phi}{V}k_B T, \tag{B5}$$

which, for purely tetrafunctional junctions, yields the expression given in Eq. 8.

The number of points at which two chains overlap is proportional, roughly, to the square of the total number of monomers incorporated into polymer, $S_\chi \approx (\Delta C)^z$, where $z = 2$ for "phantom chains" that can pass through each other, and $z = 9/4$ when "excluded volume" is taken into account (de Gennes, 1979). If chains are cross-linked by an actin-binding protein such as filamin, which forms tetrafunctional junctions, the number

of effective cross-links will be given as $A = A_0K_\chi S_\chi/(1 + K_\chi S_\chi)$, where K_χ is the association constant for the cross-linking reaction. When $K_\chi S_\chi$ is small, one finds, simply, $A \approx S_\chi \approx (\Delta C)^z$, as is also the case for entanglements that are momentarily frozen in place.

The analogous probabilities for formation of junctions requiring the random overlap of more than two chains necessarily involves higher powers of ΔC. Thus, by Eq. B5, one sees that, if junctions of higher functionality are involved, g_0 might be expected to vary as $g_0 \approx (\Delta C)^{2+}(1 + f(\Delta C))$, where $f(\Delta C)$ is of order one or greater in powers of ΔC. However, no higher order terms of ΔC are apparent in the TT data shown in Fig. 3 *A*, which implies, e.g., that the bundling of F-actin filaments is not a significant factor in the generation of early increases in cell rigidity.

APPENDIX C: DERIVATION OF EQ. 16

Perhaps the simplest mathematical description of stimulus transduction by heterotrimeric G-proteins is a bulk-reaction model in which a ligand binds to a specific receptor, which, in turn, then interacts with an intact G-protein complex composed of a GDP-bound α-subunit and an associated $\beta\gamma$-dimer. This leads to the exchange of GTP for GDP and the simultaneous dissociation of the complex and release of the GTP-bound G_α subunit (Mahama and Linderman, 1994). Let [R] represent the concentration of free (unbound) receptors, let [L] be the free ligand concentration, let [C] be the concentration of ligand-receptor complexes, let [G] be the concentration of intact heterotrimeric G-protein, and let $[\alpha]$ be the concentration of activated GTP-G_α subunits. The kinetic equation for the association and dissociation of ligand-receptor complex then may be written as

$$\frac{d[C]}{dt} = k_f[L][R] - k_r[C]. \tag{C1}$$

Here, k_f and k_r are forward and reverse rate constants for the reaction, and $[L]_{tot} = [L] + [C]$ and $[R]_{tot} = [R] + [C]$ are, respectively, the total concentrations of ligand and receptor. An analogous equation for the concentration of GTP-bound "free" G_α subunit is

$$\frac{d[\alpha]}{dt} = k_c[C][G] - k_i[\alpha], \tag{C2}$$

where k_c is a rate constant expressing the overall reaction involving association of the ligand-bound receptor with a heterotrimeric G-protein and resulting phosphorylation and dissociation of the complex. The coefficient k_i is a rate constant for the hydrolytic conversion of GTP-G_α subunits to GDP-G_α subunits. The latter are assumed to reassociate instantaneously (on the time scale of the overall G-protein reaction cycle) with $\beta\gamma$-subunits to form an intact $\alpha\beta\gamma$ heterotrimeric complex, so the conservation of α-subunits may be expressed as $[G] + [\alpha] = \text{constant} = [G]_{tot}$.

If one defines the dissociation constant K_D as $K_D = k_r/k_f$, then, from Eq. C1, one finds that the steady-state concentration of ligand-receptor complex is

$$[C]_{ss} = K_D^{-1}[L]_{ss}[R]_{ss} \approx K_D^{-1}[L]_{tot}([R]_{tot} - [C]_{ss}), \tag{C3}$$

where we assume that the concentration of ligand in the bathing solution is much greater than the concentration of bound ligand. Consequently, $[C]_{ss}$ may be expressed as

$$[C]_{ss} = \frac{[L]_{tot}[R]_{tot}}{K_D + [R]_{tot}}. \tag{C4}$$

Similarly, from Eqs. C2 and C4, one finds that the steady-state concentration of free GTP-G_α subunits may be expressed as

$$[\alpha]_{ss} = \frac{[G]_{tot}[C]_{ss}}{K^* + [C]_{ss}} = \frac{[G]_{tot}[R]_{tot}X}{([R]_{tot}/K^* + 1) + X}, \tag{C5}$$

where K^* and X are defined as $K^* = k_c/k_i$ and $X = [L]_{tot}/K_D$, respectively. Finally, when one defines γ_1, γ_2, and Y as

$$\gamma_1 = \frac{1}{[G]_{tot}}\left(1 + \frac{K^*}{[R]_{tot}}\right); \qquad \gamma_2 = \frac{K^*}{[G]_{tot}[R]_{tot}}; \qquad Y = \ln X = \ln([L]_{tot}/K_D), \tag{C6}$$

one obtains the simple form given in Eq. 16, viz.,

$$[\alpha]_{ss} = \frac{1}{\gamma_1 + \gamma_2 e^{-Y}}. \tag{C7}$$

From this expression one observes that $[\alpha]_{ss} \to 0$ when $X = [L]_{tot}/K_D$ is very small, because in this case the quantity $\exp(-Y)$ is large. Conversely, when X is large, the factor $\exp(-Y)$ is small and $[\alpha]_{ss} \to \gamma_1^{-1}$. However, regardless of the values of γ_1 and γ_2, numerical evaluation of Eq. C7 indicates that the dependence of $[\alpha]_{ss}$ on Y is linear over ~1.5–2 log units.

If, in Eq. C1, the dependence on [L] were to be expressed as $[L]^n$, it would follow that $[\alpha]_{ss}$ would be given as

$$[\alpha]_{ss} = \frac{G}{K^* \cdot R^{-n}(1 - e^{-Y})^n + 1}, \tag{C8}$$

which reduces to Eq. C7 if $n = 1$. In comparison with behavior based on Eq. C7, when the index n is greater than 1, one finds that the range of Y over which the transition from small values of $[\alpha]_{ss}$ to large values of $[\alpha]_{ss}$ occurs is narrowed. Values of $n > 1$ would correspond, e.g., to cooperativity in ligand-induced potentiation of receptors. In contrast, the transition is broadened if $n < 1$, corresponding, e.g., to a case in which saturation of the transduction machinery occurs.

The author thanks Drs. Liana Harvath and Amir Gandjbakhche for interesting discussions on this and related topics. He also expresses his appreciation to Ms. Ana Gonzales for her help in preparing the manuscript.

REFERENCES

Alberts, B., D. Bray, J. Lewis, M. Raff, K. Roberts, and J. D. Watson. 1994. Molecular Biology of the Cell, 3rd Ed. Garland, New York.

Bray, D., J. Heath, and D. Moss. 1986. The membrane-associated "cortex" of animal cells: its structure and mechanical properties. *J. Cell Sci. Suppl.* 4:71–88.

Carlier, M-F., V. Laurent, J. Santolini, R. Melki, D. Didry, G-X. Xia, Y. Hong, N-H. Chua, and D. Pantaloni. 1997. Actin depolymerizing factor (ADF/Cofilin) enhances the rate of filament turnover: implication in actin-based motility. *J. Cell Biol.* 136:1307–1323.

Coates, T. D., R. G. Watts, R. Hartman, and T. H. Howard. 1992. Relationship of F-actin distribution to development of polar shape in human polymorphonuclear neutrophils. *J. Cell Biol.* 117:765–774.

de Gennes, P.-G. 1979. Scaling Concepts in Polymer Physics. Cornell University Press, Ithaca, NY.

Doi, M. A., and S. F. Edwards. 1986. The Theory of Polymer Dynamics. Clarendon Press, Oxford.

Evans, E., and B. Kukan. 1984. Passive material behavior of granulocytes based on large deformation and recovery after deformation tests. *Blood.* 64:1028–1035.

Evans, E., and A. Yeung. 1989. Apparent viscosity and cortical tension of blood granulocytes determined by micropipet aspiration. *Biophys. J.* 56:151–160.

Fechheimer, M., and S. H. Zigmond. 1993. Focusing on unpolymerized actin. *J. Cell Biol.* 123:1–5.

Ferry, J. D. 1980. Viscoelastic Properties of Polymers, 3rd Ed. Wiley, New York.

Flory, P. J. 1953. Principles of Polymer Chemistry. Cornell University Press, Ithaca, NY.

Frank, R. S. 1990. Time-dependent alterations in the deformability of human neutrophils in response to chemotactic activation. *Blood.* 76: 2606–2612.

Frank, R. S., and M. A. Tsai. 1990. The behavior of human neutrophils during flow through capillary pores. *J. Biomech. Eng.* 112:277–282.

Green, M. S., and A. V. Tobolsky. 1946. A new approach to the theory of relaxing polymeric media. *J. Chem. Phys.* 14:80–92.

Howard, T. H., and C. O. Oresajo. 1985a. The kinetics of chemotactic peptide-induced change in F-actin content, F-actin distribution, and the shape of neutrophils. *J. Cell Biol.* 101:1078–1085.

Howard, T. H., and C. O. Oresajo. 1985b. A method for quantifying F-actin in chemotactic peptide activated neutrophils: study of the effect of tBOC peptide. *Cell Motil.* 5:545–557.

Janmey, P. A., S. Hvidt, J. Lamb, and T. P. Stossel. 1990. Resemblance of actin-binding protein/actin gels to covalently cross-linked networks. *Nature.* 345:89–92.

Koutsouris, D., R. Guillet, R. B. Wenby, and H. J. Meiselman. 1989. Determination of erythrocyte transit times through micropores: influence of experimental and physicochemical factors. *Biorheology.* 26:881–898.

Machesky, L. M., P. J. Goldschmidt-Clermont, and T. D. Pollard. 1990. The affinities of human platelet and *Acanthamoeba* profilin isoforms for polyphosphoinositides account for their relative abilities to inhibit phospholipase C. *Cell Regul.* 1:937–950.

Machesky, L. M., and T. D. Pollard. 1993. Profilin as a potential mediator of membrane-cytoskeleton communication. *Trends Cell Biol.* 3:381–385.

MacKintosh, F. C., J. Käs, and P. A. Janmey. 1995. Elasticity of semiflexible biopolymer networks. *Phys. Rev. Lett.* 75:4425–4428.

Mahama, P. A., and J. J. Linderman. 1994. A Monte Carlo study of the dynamics of G-protein activation. *Biophys. J.* 67:1345–1357.

Mahama, P. A., and J. J. Linderman. 1995. Monte Carlo simulations of membrane signal transduction events: effect of receptor blockers on G-protein activation. *Ann. Biomed. Eng.* 23:299–307.

Nachmias, V. T. 1993. Small actin-binding proteins: the β-thymosin family. *Curr. Opin. Cell Biol.* 5:56–62.

Needham, D., and R. M. Hochmuth. 1990. Rapid flow of passive neutrophils into a 4 μm pipet and measurement of cytoplasmic viscosity. *J. Biomech. Eng.* 112:269–276.

Nossal, R. 1985. Network formation in polyacrylamide gels. *Macromolecules.* 18:49–54.

Nossal, R. 1988. On the elasticity of cytoskeletal networks. *Biophys. J.* 53:349–359.

Omann, G. M., R. A. Allen, G. M. Bokoch, R. G. Painter, A. E. Traynor, and L. A. Sklar. 1987. Signal transduction and cytoskeletal activation in the neutrophil. *Physiol. Rev.* 67:285–322.

Pantaloni, D., and M-F. Carlier. 1993. How profilin promotes actin filament assembly in the presence of thymosin β4. *Cell.* 75:1007–1014.

Pearson, D. S., and W. W. Graessley. 1978. The structure of rubber networks with multifunctional junctions. *Macromolecules.* 11:528–533.

Pécsvárady, Z., T. C. Fisher, A. Fabók, T. D. Coates, and H. J. Meiselman. 1992. Kinetics of granulocyte deformability following exposure to chemotactic stimuli. *Blood Cells.* 18:333–352.

Richardson, R. M., B. Haribabu, H. Ali, and R. Snyderman. 1996. Cross-desensitization among receptors for platelet activating factor and peptide chemoattractants. *J. Biol. Chem.* 271:28717–28724.

Sato, M., W. H. Schwarz, and T. D. Pollard. 1987. Dependence of the mechanical properties of actin/α-actinin gels on deformation rate. *Nature.* 325:828–830.

Shea, L., and J. J. Linderman. 1997. Mechanistic model of G-protein signal transduction: determinants of efficacy and effect of precoupled receptors. *Biochem. Pharmacol.* 53:519–530.

Sheterline, P., and J. E. Rickard. 1989. The cortical actin filament network of neutrophil leucocytes during phagocytosis and chemotaxis. *In* The Neutrophil: Cellular Biochemistry and Physiology. M. B. Hallett, editor. CRC Press, Boca Raton, FL. 141–165.

Sklar, L. A., G. M. Omann, and R. G. Painter. 1985. Relationship of actin polymerization and depolymerization to light scattering in human neutrophils: dependence on receptor occupancy and intracellular Ca^{++}. *J. Cell Biol.* 101:1161–1166.

Theriot, J. A. 1994. Regulation of the actin cytoskeleton in living cells. *Semin. Cell Biol.* 5:193–199.

Tsai, M. A., R. S. Frank, and R. E. Waugh. 1993. Passive mechanical behavior of human neutrophils: power-law fluid. *Biophys. J.* 65: 2078–2088.

Tsai, M. A., R. S. Frank, and R. E. Waugh. 1994. Passive mechanical behavior of human neutrophils: effect of cytochalasin B. *Biophys. J.* 66:2166–2172.

Wallace, P. J., R. P. Wersto, C. H. Packman, and M. A. Lichtman. 1984. Chemotactic peptide-induced changes in neutrophil conformation. *J. Cell Biol.* 99:1060–1065.

Watts, R. G., M. A. Crispens, and T. H. Howard. 1991. A quantitative study of the role of F-actin in producing neutrophil shape. *Cell Motil. Cytoskeleton.* 19:159–168.

Worthen, G. S., B. Schwab III, E. L. Elson, and G. P. Downey. 1989. Mechanics of stimulated neutrophils: cell stiffening induces retention in capillaries. *Science.* 245:183–186.

Wymann, M. P., P. Kernen, T. Bengtsson, T. Andersson, M. Baggiolini, and D. A. Deranleau. 1990. Corresponding oscillations in human neutrophil shape and filamentous actin content. *J. Biol. Chem.* 265: 619–622.

Wymann, M. P., P. Kernen, D. A. Deranleau, and M. Baggiolini. 1989. Respiratory burst oscillations in human neutrophils and their correlation with fluctuations in apparent cell shape. *J. Biol. Chem.* 264: 15829–15834.

Yeung, A., and E. Evans. 1989. Cortical shell-liquid core model for passive flow of liquid-like spherical cells into micropipets. *Biophys. J.* 56: 139–149.

Zhelev, D. V., D. Needham, and R. M. Hochmuth. 1994. Role of the membrane cortex in neutrophil deformation in small pipets. *Biophys. J.* 67:696–705.